LOCAL PARAMETERS OF AIR-WATER TWO-PHASE FLOW AT A VERTICAL T-JUNCTION

G. Monrós-Andreu, R. Martínez-Cuenca, S. Torró and S. Chiva *
Universitat Jaume I
gmonros@uji.es; rcuenca@uji.es; torro@uji.es; schiva@uji.es

ABSTRACT

Significant experimental work and modeling about vertical T-Junction as a phase separator has been done for churn and annular flows, but a survey on the literature reveals a lack of experimental data regarding bubbly flow. Therefore, the objective of this work is to expand the state of knowledge by obtaining complete data (gas and liquid) of the phase split process in bubbly flow conditions by means of conductivity needle probes and LDA, to characterize gas and liquid phases respectively. Measurements and observations of the phase split in a vertical T-Junction with equal pipe diameters (52 mm inner diameter) are reported.

KEYWORDS
Two-phase, T-Junction, vertical pipe, conductivity probes, LDA

1. INTRODUCTION

Two-phase gas-liquid flow in T-Junctions form part in a wide range of process plant (i.e. oil extraction and processing or water cooled nuclear reactors pipe systems). In gas/liquid flow splitting process at T-Junctions, the fluid momentum fluxes for each phase are important factors in the partition of the phases. When a two-phase mixture flows through a splitting T-Junction tend to separate in variable fractions at outlet branches. In case of noticeable density differences between phases, i.e. air-water mixtures, the lighter phase tends to be diverted into the side arm while heavier phase tends to flow in the inlet branch direction.

Research on phase redistribution of two-phase flows at junctions has two main motivations: one is to prevent the asymmetry in phase distribution between branches when a T-junction is used as a simple fluid divider and another is to provide effective phase separation when the T-Junction acts as a partial phase separator. For both purposes it is essential to understand and predict the degree of phase segregation and general flow behavior of the mixture at T-Junction for various operating conditions.

Most of existing methods to predict the flow separation are totally empirical or based on one-dimensional flow analysis, relying also on empirical correlations. The present state of understanding reveals the great complexity of analyzing the segregation phenomena, identifying some of the important parameters such as flow pattern [1], radial void fraction distribution [2] or branch-inlet diameter ratio [3].

A present challenge in multiphase flow is the development of proper general models for modeling through three dimensional Computational Fluid Dynamics (CDF) codes, which may open a new path for understanding and optimization. A survey on the literature reveals a lack of data with high spatial resolution, which is necessary to model validation. The utmost purpose of provided data and

*Corresponding author

presented methodology is to serve to validate those codes and models, as it provides the necessary local flow parameters.

2. EXPERIMENTAL FACILITY

As illustrated in Fig. 1, test section consists in two vertical and one horizontal Plexiglas® pipe sections with 52 mm inner diameter (ID). The three sections are connected through a T-junction port made of two mechanized parts, one of them made of Plexiglas® to enable optical access.

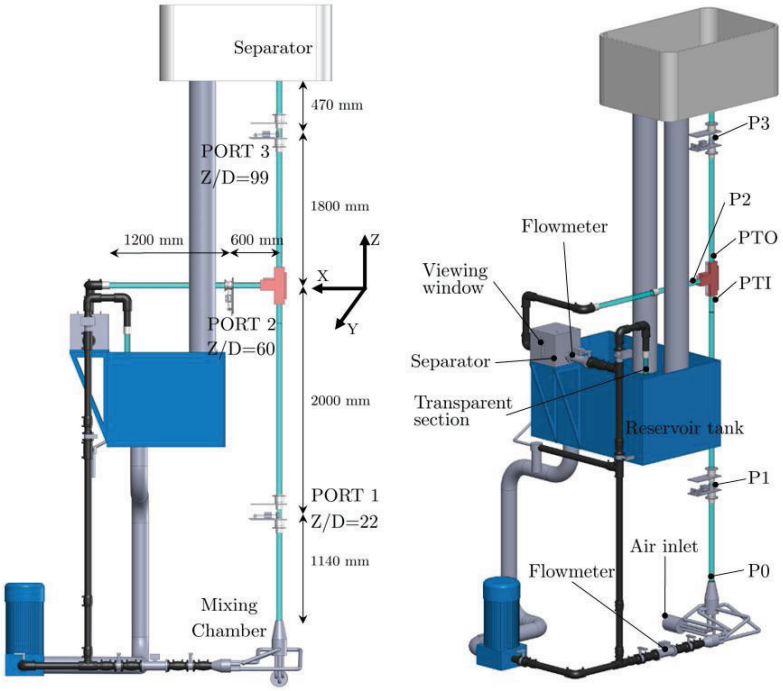

Figure 1. Schematic diagram of the experimental facility.

Operating fluids are air and purified water (conductivity 200-300 μS/m). The water is circulated by a centrifugal pump and stored in a 500L reservoir tank and is kept at a constant temperature (20°C) thanks to a heat exchanger. An air flow-meter controller (Bronckhorst EL-FLOW 250 lNpm) is used to adjust and measure the gas flow-rate. The air-water mixing is performed in a mixing chamber composed by 4 separate compartments, each one having a liquid inlet at the bottom and a gas inlet through a sparger (40 μm average porosity) which is oriented axially with the main flow. This configuration provides a quite uniform distribution of gas and liquid at the pipe inlet.

In order to measure the gas and liquid flow rates, there are installed two flow separators. The first one, located on top of the vertical section is open to atmosphere. The second separator is located downwards horizontal branch. It has interior baffles to improve the separation and a viewing window to control the water level. The air from the separator tank passes through two separator valves and a small air-reservoir tank, to smooth air pressure fluctuations, and finally through an air rotameter. To reach quasi-stationary flow and to obtain precise measure of air separated flow rate, the pressure inside the separator tank is controlled manually with the rotameter aperture until the water level (by visual inspection through tank viewing window) is kept constant during a long period of time (about 30 minutes for each run test). Liquid flow rate is measured downstream from the separator tank. A

transparent pipe section located at the outlet allows to visually inspect the flow and verify the complete phase separation, which ensures to obtain correct measurements of liquid flow rate.
The local flow parameters were measured at three measurement ports, Port 1 and Port 3 located at vertical sections at Z/D=22 and Z/D=99, and Port 2 located at horizontal branch at Z/D=60 and X/D=10 (from the center of T-junction). Gas-phase local parameters are measured using four-sensor conductivity probes, mounted on each measurement port. As Fig. 2 shows, the conductivity probes are attached to a scanning system driven by a stepper motor. This system is used to take the gas phase measurements at 16 radial locations at vertical measurements ports, where it can be assumed azimuthally homogeneity of flow distribution, as the measurement ports are far from the inlet an T-Junction. This assumption is no longer valid on the horizontal branch where the only possible assumption is the symmetry around Z axis, caused by phases stratification. The use of a rotating section on the horizontal branch (Port 2) enables the probe to be moved to any spatial location in a XY plane in the horizontal branch. The constructed rotating section allows the rotation of whole scanning probe systems in 30º steps, performing the 16 radial location scan with the probe. At each flow condition the probes are moved to 135 distinct spatial locations (Fig. 2).

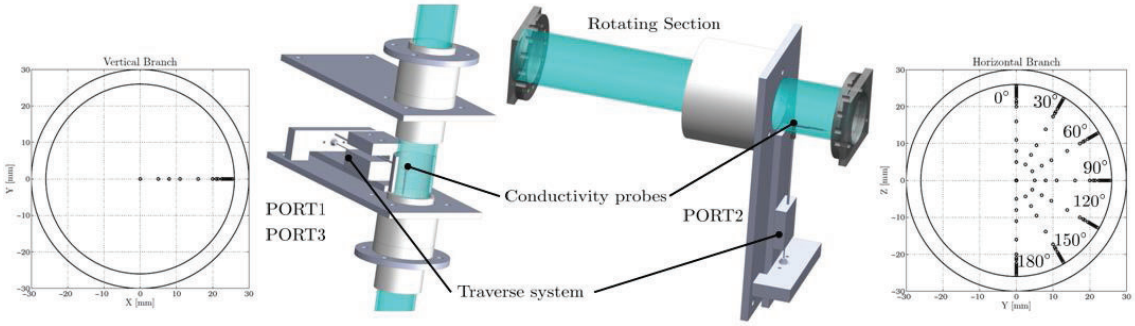

Figure 2. Detail of measurement ports and measurement points.

All probe voltage signals are simultaneously recorded over 15 seconds for all experimental conditions at a 60 kHz sampling rate by using a high-speed acquisition board (NI SCXI-1000).
In order to measure the liquid local parameters inside the T-junction, the Laser Doppler Anemometry (LDA) technique is used. The LDA equipment is composed of a 0.5 W Ar^{+} Ominichrome Laser, a beam separator (Dantec Fiberflow), a signal processor (Dantec FVA 58N40) and acquisition software (Floware). Two laser lines are used (488 and 512 nm with a focal spot of approximately 1mm width and 2 mm depth. Round polyamide seeding particles (mean diameter of 5μm) are dispersed in the water in such a concentration that the sampling frequency are over 1 kHz for single-phase conditions.
Additional equipment is used to measure average flow properties and to ensure the stationary conditions of the mean flow. Thus, water temperature in the reservoir tank and downstream from mixing chamber, is monitored by using PT100 thermocouples.
Pressure is measured with pressure transducers with a range 0-1 bar for P0 and P1 locations, 0-0.6 Bar for PTI, PTO and P2 locations and 0-0.25 bar for P3 location (all transducers with a 0.1% relative error). Probe positioning, flow rate setup and variable measurements are implemented and automated in LabView® environment, it permits to obtain high reproducibility on the experiment setup and results.

3. FOUR-SENSOR PROBE METHODOLOGY

The four-sensor probe is basically a phase identifier with four effective local measurement points close to each other. It consists of four sensors made of insulated copper wires, with a diameter of 0.2 mm. The probe is connected to a power supply with a fixed voltage, due to the large difference in conductivity between liquid phase and gas phase. The impedance signal of each sensor acquired rises sharply when a bubble passes through the sensor tip.

The tip of the front common sensor and the three rear tip sensors are adjusted for a typical distance of approximately 2 mm in the main flow direction. It is important to establish a three-dimensional Cartesian coordinate, with its origin at the front sensor tip, to obtain the distance vectors between front and rear tips ($\overrightarrow{s_{01}}$, $\overrightarrow{s_{02}}$, $\overrightarrow{s_{03}}$), as it is depicted in Fig. 3. Based on these sensor tip coordinates, all required geometrical parameters of the four-sensor probe can be obtained, in order to compute local flow parameters.

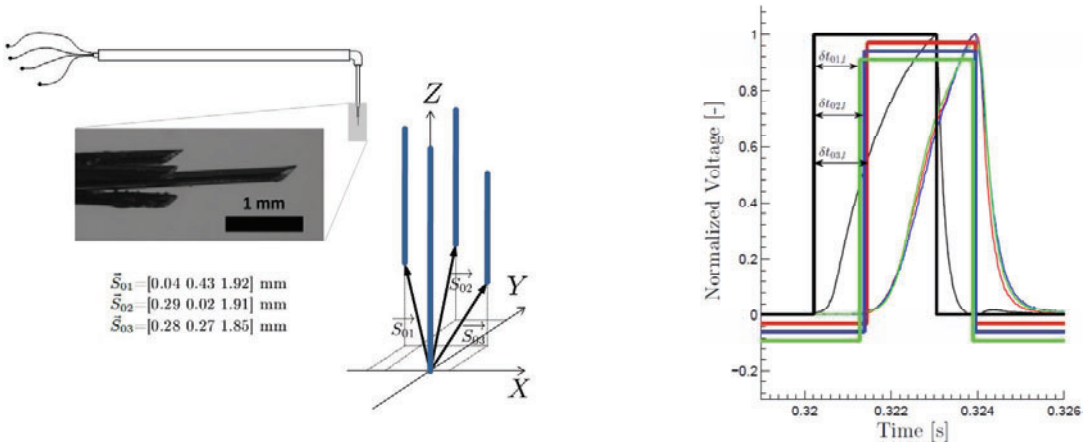

Figure 3. Probe geometry (left) and example of single bubble passing through four-sensor conductivity probe tips: Raw signals (thin lines), regenerated square signals (thick lines) and time delays between signals (right).

The signal output from the optical probe is different from the ideal two-state square-wave, caused by the finite size of the sensors and the time delay needed to wet or rewet the flat tips,. To regenerate the ideal square-wave signal, a threshold method proposed by Barrau et al. [4] combined by method proposed by Dias and Rosa [5] was used to process the raw probe signals and to extract required information from the two phases. The raw signal obtained from the four-sensor probe and the regenerated square signal by the above-mentioned methods are displayed in Fig. 3, in which the high and low voltages represent the gas and the liquid phase respectively.

4. EXPERIMENTAL RESULTS: LOCAL FLOW PARAMETERS

In this study, two conditions of two-phase flow have been tested. The experimental conditions test matrix are summarized in Table I. Superficial velocities for liquid phase (j_L) at z/D=0 (inlet) and horizontal branch are listed. Local superficial gas velocity (j_G) is calculated based on gas volumetric flow rate measurement and the pressure at Z/D=22 (Port1). Area-averaged values are denoted by < >. Table I also includes the area-averaged void fraction measured with the four-sensor conductivity probe, as it is considered an important factor to define the experimental condition.
Pressure values for complete characterization of flow conditions are listed in Table II. It should be noted that due to the complexity and fluctuations involving a phase split in a T-Junction, maximum deviations of 10 mbar have been registered during tests in the pressures listed, which are considered in an acceptable range of accuracy.

Table I. Experimental test conditions (Flow rates)

Run	Q_{water} (inlet) [lpm]	j_L (inlet) [m/s]	Q_{water} (Horizontal Branch) [lpm]	j_L (Horizontal Branch) [lpm]	Q_{air} (Port 1) [lNpm]	j_G (Port 1) [m/s]	$\langle\alpha\rangle$ (Port 1) [%]
R1A	250.35	1.95	169.36	1.32	21.5	0.15	8.94
R1B	260.13	2.03	154.94	1.21	58.5	0.40	19.01

Table II. Experimental test conditions (Pressure)

Run	P0 [mBar]	P1 [mBar]	PTI [mBar]	P2 [mBar]	PTO [mBar]	P3 [mBar]
R1A	539.80	425.17	264.44	237.98	238.10	86.41
R1B	503.91	398.06	249.04	219.98	221.54	81.27

Both experimental conditions (R1A and R1B) have been repeated for each angle variation of the rotating section in the horizontal branch (7 rotations). Therefore, experimental results corresponding to the measurement ports located at vertical sections (Port 1 and Port 2) include the mean and deviation between repetitions.

In the following sections, the mathematical foundations to calculate the main parameters needed to characterize the gas phase, such as the void fraction, the velocity of the bubble's interfaces, the bubble frequency and the interfacial area concentration, are presented.

4.1. Void Fraction Measurements

The mean local volume fraction of the bubbles (or time-averaged void fraction, α) at the position of the probe can be well estimated from the conductance signal, as it can be determined by the fraction of time that the sensor is exposed to gas phase over the total sampling time.

Fig. 4 shows 3D and 2D profiles of void fraction measurements at horizontal branch (Port 2) for R1A and R1B, where the radial local values at each port rotation (from 0 to 180º) have been radially interpolated. These void fraction distributions show a clear but different stage of stratification in both flow conditions, where the disperse phase tend to move towards the top of the section. However, it can be observed a significant value of void fraction remains close to the bottom wall of the pipe, it stresses the fact that probe locations and port rotations must cover at least one half of the cross-section area for accurate local parameters measurement.

In Fig. 5 can be observed the characteristic wall-peak profiles from bubbly flow pattern in vertical sections. Gas phase separation in the T-Junction is clearly observed: for both conditions the remaining void fraction at Port 3 is almost half from Port 1.

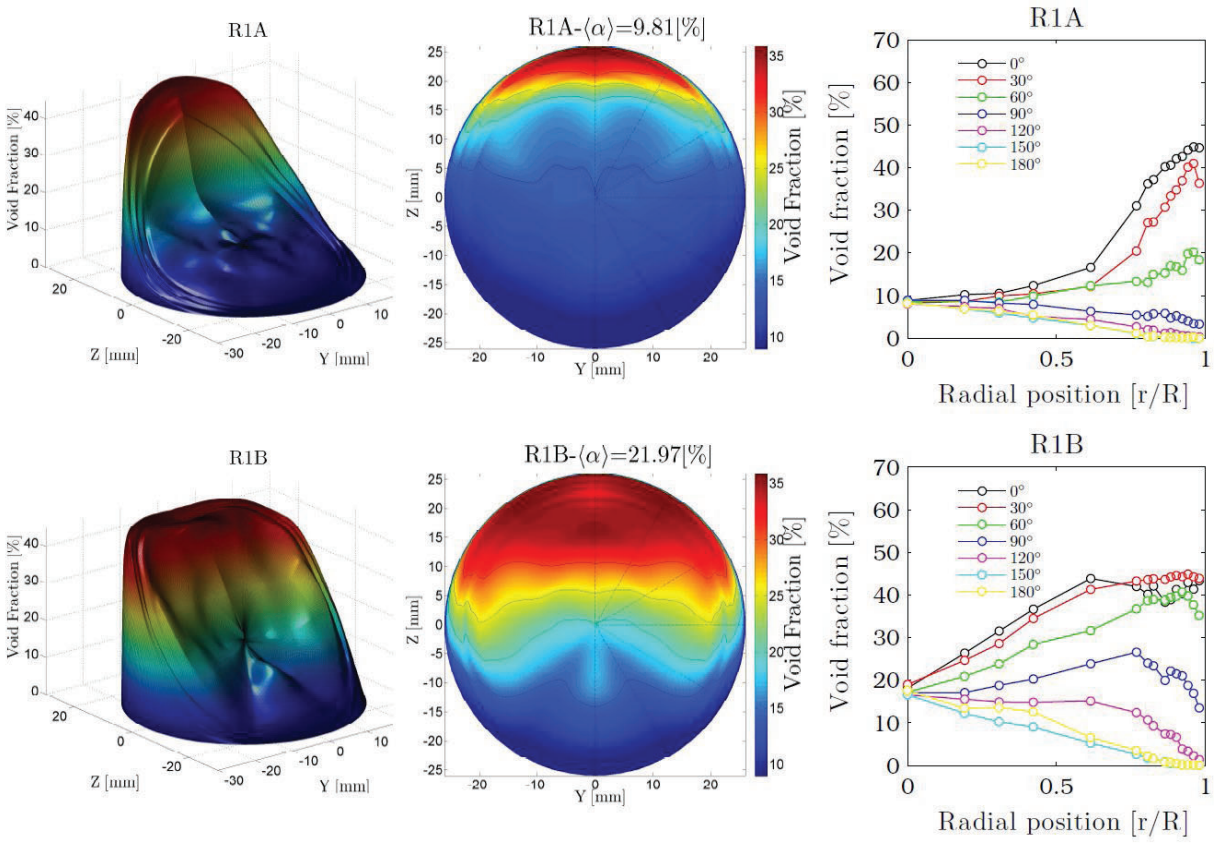

Figure 4. Void fraction measurements at horizontal branch (Port 2) for R1A (top) and R1B (bottom).

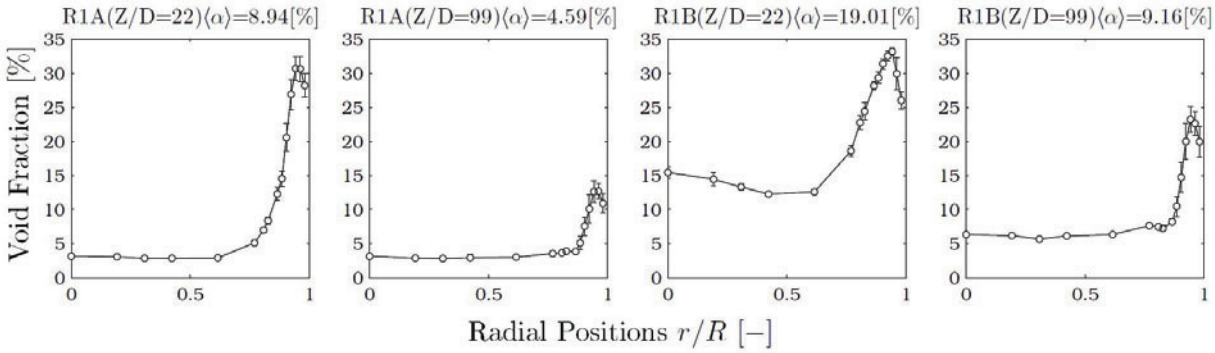

Figure 5. Void fraction measurements at Port 1 and Port 3 for R1A (left) and R1B (right).

4.2. Interfacial velocity

The time delay between the paired signals allow the calculation of the interfacial velocities for the individual bubbles. If each bubble is labeled with the sub-index *l*, then the *l-th* corresponding bubble interfacial velocity, $\overrightarrow{V_{0K,l}}$ can be computed from the three independent tip-position vectors, $\overrightarrow{s_{0K,l}}$. First, the following velocity vectors are constructed:

$$\overrightarrow{V_{0K,l}} = \frac{\overrightarrow{s_{0K,l}}}{\delta T_{0K,l}}, k = 1,2,3 \quad (1)$$

Where δT_{0K} stands for the time delay between the rising time of central tip and the rising time of rear tip k. The interfacial velocity (parallel to the flow direction) can be estimated as:

$$\overrightarrow{V_{i,l}} = \frac{|\overrightarrow{V_{01,l}}|+|\overrightarrow{V_{02,l}}|+|\overrightarrow{V_{03,l}}|}{3} \quad (2)$$

The average value of interfacial velocity is obtained from the best-fitting distribution of $V_{i,l}$ data. Even in a vertical upward flow configuration the velocity of air bubbles are not purely axial but have small lateral components as well. Wu et al [6] demonstrated that bubbles with significant lateral motion can cause the surface of a bubble to strike almost simultaneously the front and rear sensor tips (like piercing bubble near to the edge), so it produces a very small time delay and related overestimation of axial velocity component. These bubble lateral motion can also increase the number of missing bubble (bubbles which touch the front sensor but miss one or more rear sensor tips). In order to overcome the velocity overestimation problem, in this work it is suggested the use of two velocity thresholds (upper and lower) based on known averaged superficial velocity of liquid phase (j_L) in order to overcome those problems. Threshold limits proposed in Eq. 3 are wide enough just to prevent extreme values affecting averaged velocity (under 14% of total computed bubbles for testes conditions).

$$0.2j_L < V_{0K,l} < 5j_L \quad (3)$$

This procedure is used to discard abnormal velocities and match the square-wave signal for each effective bubble detected. A minimum of 200 velocity samples are used to perform the fitting and obtain the local velocity.

Interfacial velocity in the flow direction measured in the horizontal branch (Port 2) is shown in Fig. 6. It can be observed the lower velocity values near the top wall of the section, where the bubbles are accumulated due buoyancy. Also the typical large velocity gradients near wall can be observed.

Fig. 7 shows the effect of liquid phase separation over interfacial velocity measured in the vertical sections. As it can be seen, a noticeable decrease in interfacial velocity between Port 1 and Port 3 is observed. For both experimental conditions, measurements in Port 3 show the typical bubble flattening effect over interfacial velocity profiles, characteristic of bubbly flow patterns with moderate liquid flow rates and low void fractions.

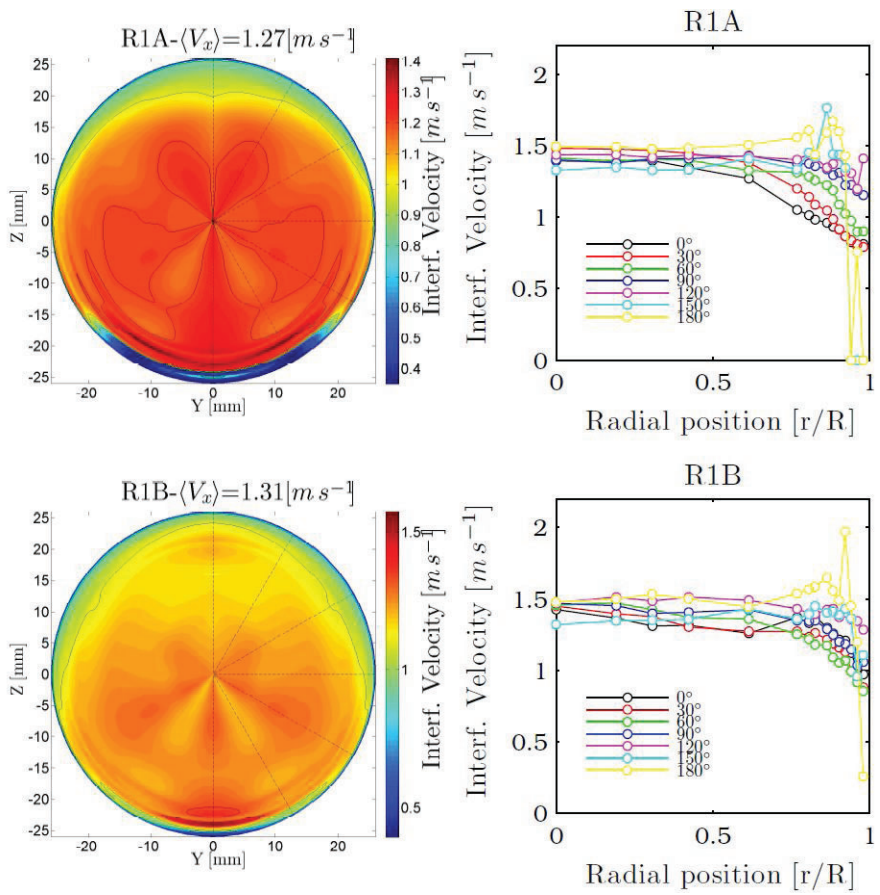

Figure 6. Interfacial velocity measurements at horizontal branch (Port 2) for R1A (top) and R1B (bottom).

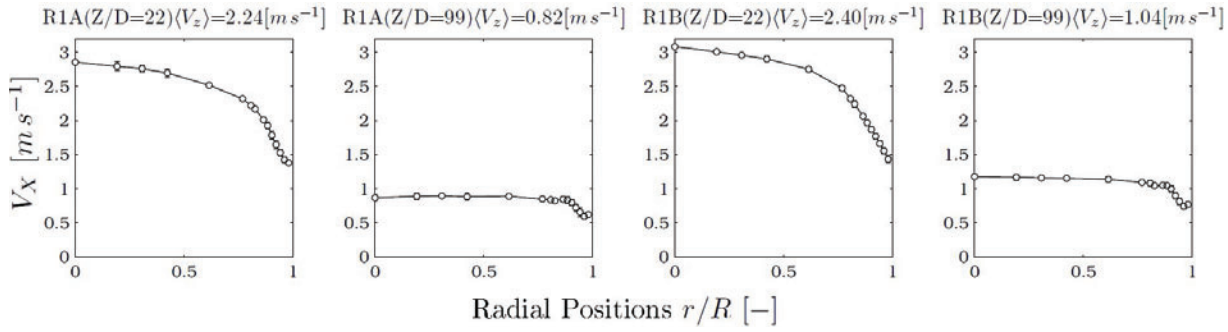

Figure 7. Interfacial velocity measurements at Port 1 and Port 3 for R1A (left) and R1B (right).

4.3. Interfacial Area Concentration (IAC)

The IAC is defined by the total interfacial area per unit mixture volume. Up to now, several investigations and experimental measurements have been carried out using four sensor probe methodology, proving the consistency of this method for IAC measurements. From the pioneer work of Kataoka and Ishii [7] on the local interfacial area derivation from velocity measurements, Kim et al. [8] proposed a miniaturized probe

and made it capable of measuring both large and small bubbles. Shen et al. [9] and Shen and Nakamura [10] proposed an explicit equation for the instantaneous local interfacial area and local interfacial velocity using four sensor conductivity probes, which take into account both receding and oncoming interfaces. Then, local values of IAC can be calculated as:

$$\bar{a}_i^t = \frac{1}{\Omega} \cdot \sum_{l=1}^{2N_t} \sqrt{\frac{{D_{01l}}^2 + {D_{02l}}^2 + {D_{03l}}^2}{{D_0}^2}} \tag{4}$$

Where N_t denotes the measured bubble number within the total sampling time Ω, and D_0, D_{01l}, D_{02l} and D_{03l} are the basic and directional determinants related to the four-sensor probe, totally determined by the three rear sensor tip coordinates referenced to front sensor tip coordinates and the time delays between square-wave signals (Fig. 2). These directional determinants are expressed by:

$$D_0 = \begin{vmatrix} x_1 & y_1 & z_1 \\ x_2 & y_2 & z_2 \\ x_3 & y_3 & z_3 \end{vmatrix}$$

$$D_{01l} = \begin{vmatrix} \Delta t_{01l} & y_1 & z_1 \\ \Delta t_{02l} & y_2 & z_2 \\ \Delta t_{03l} & y_3 & z_3 \end{vmatrix};\ D_{02l} = \begin{vmatrix} x_1 & \Delta t_{01l} & z_1 \\ x_2 & \Delta t_{02l} & z_2 \\ x_3 & \Delta t_{02l} & z_3 \end{vmatrix};\ D_{03l} = \begin{vmatrix} x_1 & y_1 & \Delta t_{01l} \\ x_2 & y_2 & \Delta t_{02l} \\ x_3 & y_3 & \Delta t_{03l} \end{vmatrix} \tag{5}$$

As interfacial velocity, time-local averaged IAC considers only effective interfaces (detected by the four sensor tips) and can be computed with Eq. (4). For missing bubbles/interfaces it is not possible to measure their velocity and therefore their contribution to IAC, and there is no accurate theoretical way to evaluate them in the measurement. In the classical procedure to overcome this problem in bubbly flow, the missing bubbles/interfaces are treated as if they possess the average value of IAC. Wu and Ishii [11] and Le Corre and Ishii [12] found numerically that this approach underestimates the real value of expected IAC, considering the fact that missing bubbles are generally the smallest bubbles or they are caught in the edge, and these ones provides the major contribution to IAC.

In this work , the results for the time-local averaged IAC were corrected by the method proposed by Le Corre and Ishii [12]:

$$a_{i,REAL} = \frac{1}{\sqrt{1-\sqrt{2.4R_N - 1.5R_N^2}}} \cdot a_{i,EFF} \tag{6}$$

Where $a_{i,REAL}$ and $a_{i,REAL}$ are the corrected time-local averaged IAC and the time-local averaged IAC from computed bubbles/interfaces. The correction method only takes into account the bubble missing ratio, R_N. Fig. 8 shows the different IAC distribution in horizontal branch cross-section. Lower values of IAC at top section in R1B stress the fact that bigger bubbles are formed due stratification, with lower contribution to IAC than small bubbles. Intermittent (plug) pattern is observed at R1B condition. Fig. 9 shows the IAC profiles in vertical sections. As expected, wall-peaked profiles are obtained as the major contribution of IAC is produced where the bubble density (or void fraction) is higher (Fig. 5).

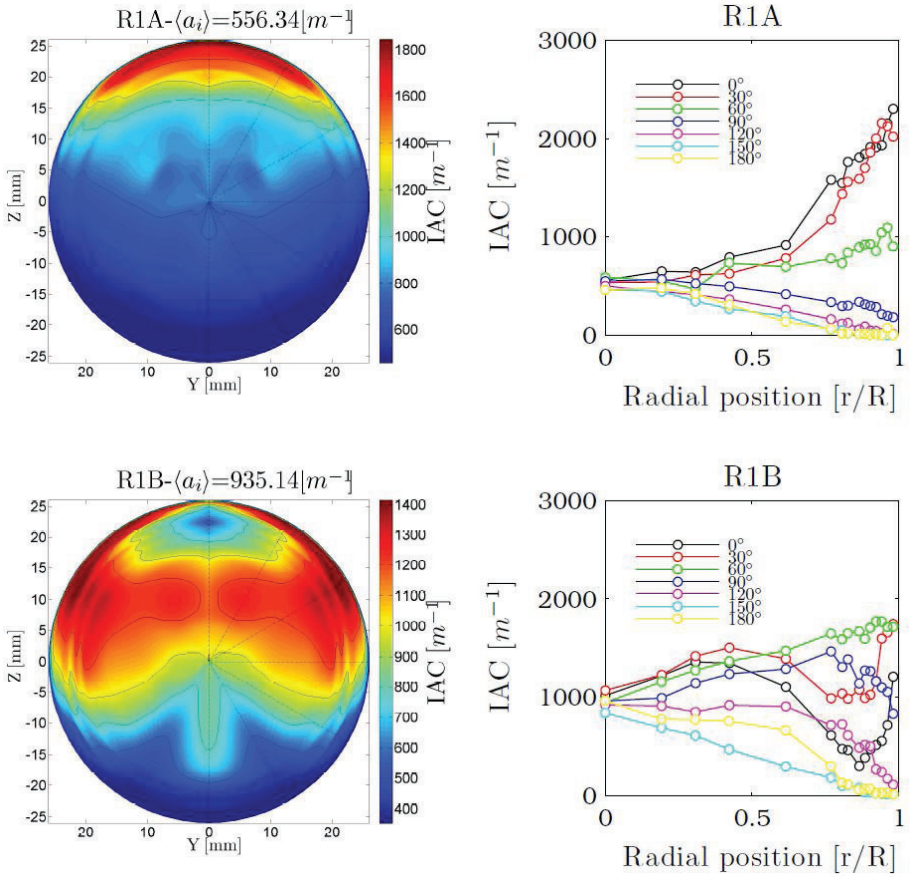

Figure 8. IAC measurements at horizontal branch (Port 2) for R1A (top) and R1B (bottom).

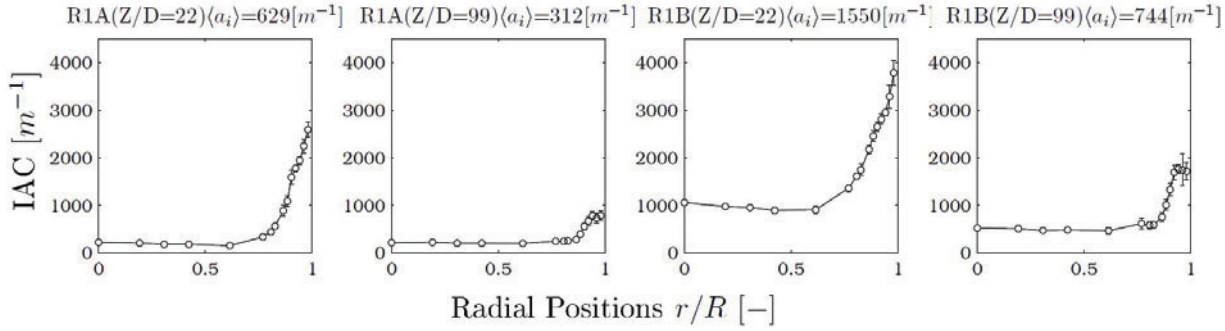

Figure 9. IAC at Port 1 and Port 3 for R1A (left) and R1B (right).

4.3. Bubble Frequency

The bubble frequency at each local point is computed as the number of bubbles detected per unit time by the front sensor of four-sensor conductivity probe. This parameter provides, in conjunction with local void fraction, qualitative information about bubble coalescence and breakage phenomena. In Fig. 10, top of the cross section for condition R1B shows a decreasing value of bubble frequency compared with the surroundings. This fact suggests, as Fig.8, that coalescing processes are happening, confirmed by

intermittent flow observed at this condition. Fig. 11 shows local bubble frequency profiles at vertical section. It can be noticed that those profiles have the same shape as their corresponding void fraction profiles (Fig. 5). This fact suggests that coalescence and breakage phenomena is not rather important in vertical sections for considered experimental conditions.

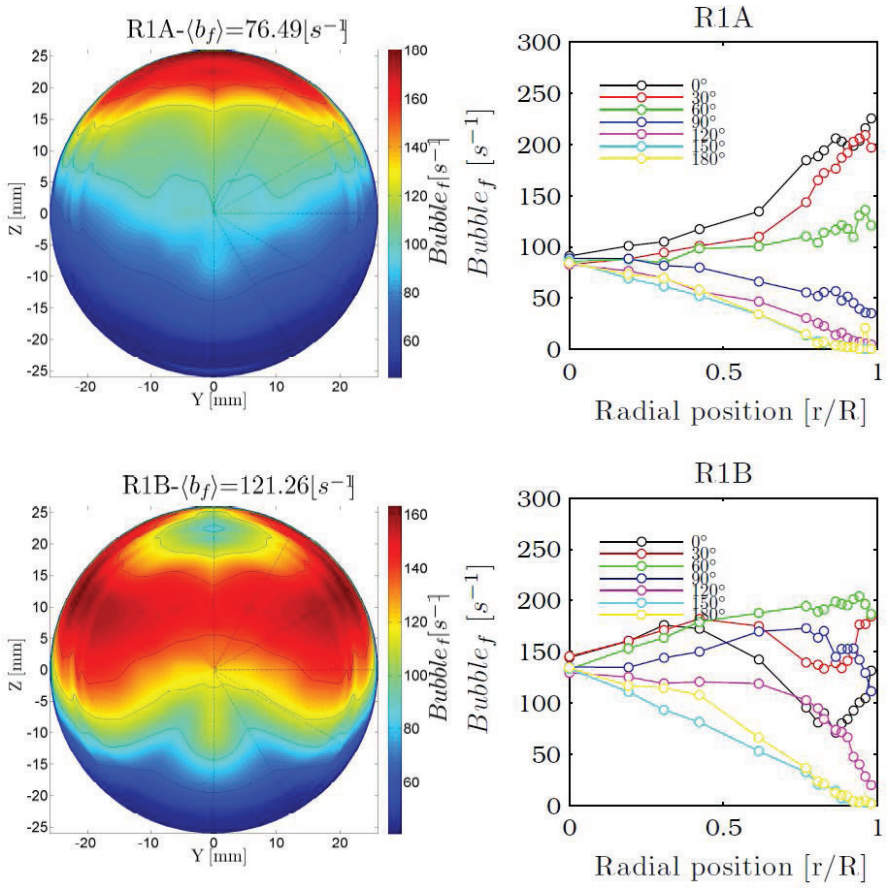

Figure 10. Bubble frequency measurements at horizontal branch (Port 2) for R1A (top) and R1B (bottom).

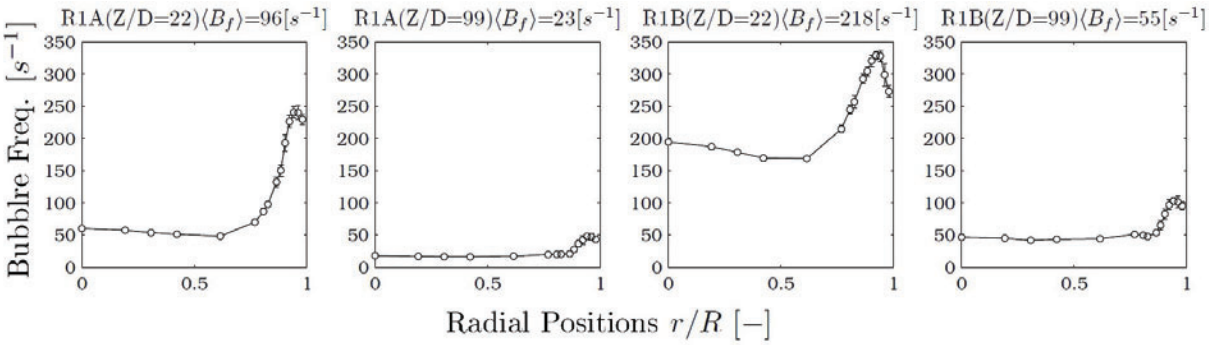

Figure 11. Bubble frequency at Port 1 and Port 2 for R1A (left) and R1B (right).

4.3. Liquid Velocity Measurements in the T-Junction

In order to quantify the liquid velocity in the splitting region, six measurements are performed around the T-Junction center for each condition by using LDA. The processed raw velocity signals provide the components of the velocity in ZX plane, the estimation of turbulent intensity (TI) and turbulent kinetic energy (TKE).

Fig. 12 shows the air distribution in the T-Junction during the phase separation process and liquid velocity vectors in the measured positions (A, B, C, D, E and F), providing information about the split process (noticeable velocity decay from D to B) and the evolution of the liquid core (vector orientation and magnitude of A, C, E and F). The increment of injected gas fraction between experimental conditions has a noticeable influence over liquid parameters.

Values of local liquid parameters mentioned above are shown in Table III. The IT values highlight the complexity of the splitting process, as it is extremely turbulent in the horizontal branch direction. Those extreme IT values can be explained by the high fluctuations observed in the liquid core.

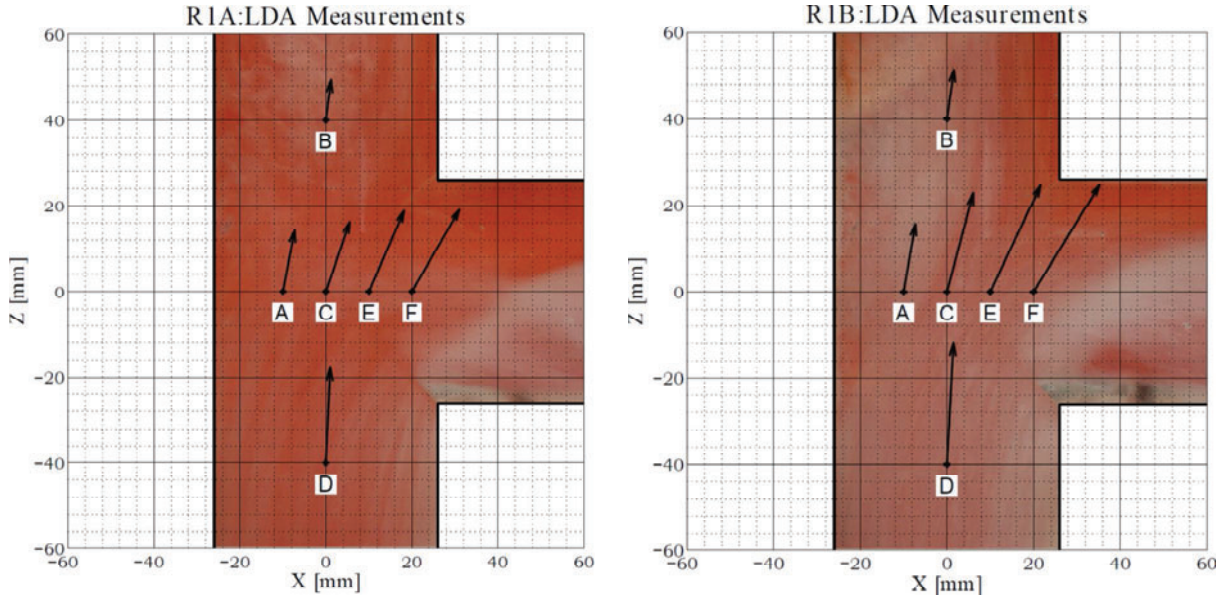

Figure 12. Liquid velocity measurements inside T-Junction, velocity modulus scaled 1:100.

Table III. Liquid local flow parameters

Location	V_x [m/s] R1A/R1B	V_z [m/s] R1A/R1B	IT_x [%] R1A/R1B	IT_z [%] R1A/R1B	TKE [m^2/s^2] R1A/R1B
A	0.30/0.3	1.58/1.74	532.22/105.54	24.12/37.85	0.10/0.32
B	0.13/0.18	1.04/1.27	199.45/197.45	57.65/60.93	0.25/0.41
C	0.61/0.67	1.80/2.53	16.45/22.71	7.14/7.79	0.02/0.04
D	0.11/0.16	2.46/3.11	48.96/99.12	3.22/6.14	0.01/0.05
E	0.90/1.29	2.08/2.73	7.22/37.35	6.30/20.55	0.01/0.39
F	1.20/1.69	2.11/2.74	5.96/37.44	5.41/26.68	0.01/0.67

5. VALIDATION

In order to verify the accuracy of the local four sensor probe measurements, the area averaged quantities, obtained by integrating the local flow parameters over the flow, have been compared with those obtained by the rotameter (horizontal branch) and by the flow controller (inlet). The air flow rates from probes are calculated based on void fraction and local gas velocity measured in the experiments by integration over the cross-section (Eq. 7). Air flow rate values obtained are listed in Table IV.

$$Q_{air} = 2\pi \int_0^R \alpha(r)V(r)r\,dr \tag{7}$$

Table IV. Air flow rate comparison. Values obtained with flow meters and four sensor probes.

Air Flow [lpm]	Rotameter [lpm] R1A	Probes [lpm] R1A	E_r [%]	Flow Controller [lpm] R1B	Probes [lpm] R1B	E_r [%]
Inlet	19.06	17.65	7.40	50.90	50.05	1.70
Horizontal Branch	17.47	14.45	17.29	48.46	35.81	26.10
Vertical Branch	6.04	4.54	24.83	14.21	11.64	18.09

The averaged and maximum relative deviations of air flow-rate listed in Table IV, between the four-sensor probes and rotameter or flow controller are 13.75% and 26.10%, so a very good agreement has been achieved for both flow conditions, as can it can be compared in the literature for similar works involving two-phase flow area-avergaed based validations [10], [14].

6. CONCLUSIONS

Methodology involving four-sensor conductivity probe was applied to the measurement of various key local parameters for an upward two-phase flow system with a vertical splitting T-Junction. Therefore, instantaneous local parameters of both gas and liquid phases were obtained, including the void fraction, interfacial velocity, IAC and bubble frequency for disperse phase and liquid velocity, turbulent intensity and turbulent kinetic energy for the continuous phase.

In addition, the measurements for void fraction and axial interfacial velocity component were checked against the void fraction measurements using the superficial gas velocity measurement using gas flow meters at two measurement ports. A remarkable agreement was found, considering the complexity of performing simultaneous measurements in two very different flow patterns, horizontal and vertical upward flow, which flow structure are influenced by the phase segregation in a T-Junction.

As future work, further experimental work should be conducted involving local measurements performed across the entire horizontal branch in order to obtain the local parameters evolution with the horizontal flow development and also local measurements in both phases inside the T-Junction, in order to fully characterize the complex flow behavior in this element.

ACKNOWLEDGMENTS

This work has been founded by the project ENE2010-21368-C02-02, financed by the Ministerio de Economía y Competitividad (Spain). G. Monrós-Andreu gratefully acknowledges a FPI-2011 predoctoral scholarship, from Ministerio de Economía y Competitividad.

REFERENCES

1. Azzopardi, B. J., "The effect of flow patterns on two-phase flow in a T junction". International Journal of Multiphase Flow, **8**(0301-9322), pp. 491–507. (1982).
2. Azzopardi, B. J., "The effect of the side arm diameter on the two-phase flow split at a tee junction". *Int. J. Multiphase Flow*, **10**, pp. 509-512(1984).
3. Hervieu, E. "Ecoulement monophasique et diphasique bulles dans un branchement en té Thèse de docteur de l'INP. (1988)
4. E. Barrau, C. Poupot, and A. Cartellier, "Single and double optical probes in air-water two-phase flows : real time signal processing and sensor performance", *Int. J. Multiphase Flow*, vol. **25**, pp. 229–256 (1999).
5. S. G. Dias, F. A. Franc, and E. S. Rosa, "Statistical method to calculate local interfacial variables in two-phase bubbly flows using intrusive crossing probes," *Int. J. Multiphase Flow*, vol. **26**, pp. 1797–1830(2000).
6. Q. Wu, K. Welter, D. McCreary, and J. N. Reyes, "Theoretical studies on the design criteria of double-sensor probe for the measurement of bubble velocity," *Flow Meas. Instrum*., vol. **12**(1), pp. 43–51,(2001).
7. I. Kataoka, M. Ishii, and A. Serizawa, "Local formulation and measurements of interfacial area concentration in two-phase flow. " *Int. J. Multiphase Flow*, vol. **12.4**, pp. 505-529,(1986).
8. S. Kim, X. Y. Fu, X. Wang, and M. Ishii, "Study on interfacial structures in slug flows using a miniaturized four-sensor conductivity probe," *Nucl. Eng. Des.*, vol. **204**(1–3), pp. 45–55, (2001).
9. X. Shen, Y. Saito, K. Mishima, and H. Nakamura, "Methodological improvement of an intrusive four-sensor probe for the multi-dimensional two-phase flow measurement," *Int. J. Multiph. Flow*, vol. **31**(5), pp. 593–617, (2005).
10. X. Shen and H. Nakamura, "Local interfacial velocity measurement method using a four-sensor probe," *Int. J. Heat Mass Transf.*, vol. **67**, pp. 843–852, (2013).
11. Q. Wu and M. Ishii, "Sensitivity study on double-sensor conductivity probe for the measurement of interfacial area concentration in bubbly flow," *Int. J. Multiphase Flow,* vol. **25**(1999).
12. J.-M. Le Corre and M. Ishii, "Numerical evaluation and correction method for multi-sensor probe measurement techniques in two-phase bubbly flow," *Nucl. Eng. Des.*, vol. **216** (1–3), pp. 221–238,(2002).
13. Shen, X., Hibiki, T., & Nakamura, H. "Developing structure of two-phase flow in a large diameter pipe at low liquid flow rate". *International Journal of Heat and Fluid Flow*, vol. **34**, pp. 70–84, (2012)